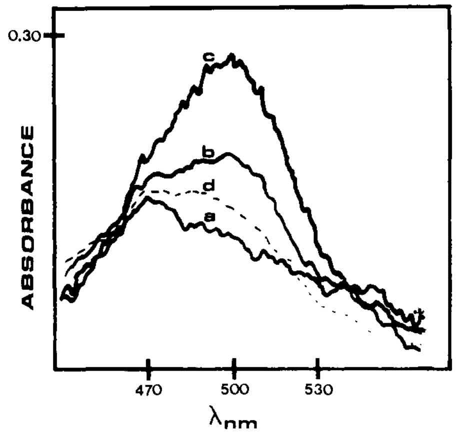

Figure 1. Appearance of carbonyl ylides IIa and IIb after photolysis of Ib in acetonitrile: (a) <50 ps; (b) 180 ps; (c) 9.1 ns; (d) (---) 125 ns.

50 ps some carbonyl ylide appears with λ_{max} at 471 nm which corresponds to IIa, the symmetry-forbideen product! Within a few nanoseconds IIb appears ($1/k$ = 320 ps, λ_{max} = 497 nm) and then decays with a lifetime of ~40 ns. At 125 ns (by which time most of IIb has decayed) the same amount of IIa remains as was present at 50 ps. This result indicates that most of the IIa formed by photolysis of Ib in acetonitrile is formed within 50 ps and suggests path A (formation of IIa from the unrelaxed excited state $^1Ib_v{}^*$) is the major source of the "forbidden" product in this case. Further analysis of the data reveals that IIa is the major product to appear in the first 50 ps (>90%). Path A simply indicates a loss of orbital symmetry control due to carbonyl ylide formation from a vibrationally excited state. We might anticipate that such a path would give similar amounts of IIa and IIb (possibly favoring the more stable ylide IIb), but we observe mostly IIa formation. It seems that the fast process leading to carbonyl ylide occurs stereospecifically in a conrotatory fashion. One explanation is that IIa arises via an upper electronic excited state of Ib from which conrotatory opening is allowed. In this case the upper excited state would have to be the result of a two-photon absorption process. This possibility is eliminated by the observation that the ratio of IIa to IIb (after photolysis of Ib in acetonitrile) is independent of laser power. Furthermore the amount of ylide formed from Ib is linear with laser power (determined over an 8-fold range of power).

It seems that the excess energy from 266-nm excitation of Ib causes efficient population of a vibrational level which is strongly coupled to the motion leading to carbonyl ylide. The 0,0 band for Ib occurs at 271 ± 3 nm[5] which results in 800 to 3100 cm^{-1} of excess energy being added by the 266-nm excitation. The oxirane ring of Ib has three infrared active absorptions between 850 and 1250 cm^{-1} which indicates that the excess energy added by the 266-nm excitation could reasonably be expected to excite some oxirane ring vibrations.[14]

Establishment that strongly coupled vibration levels can control the course of concerted reactions would help explain in some instances why photochemical reactions generally occur with less stereospecificity than thermal reactions. Future plans to examine this phenomenon include the study of wavelength and temperature effects on the ratio of IIa and IIb. Also, faster time resolution experiments will help elucidate the actual source of stereochemical loss.

Acknowledgment. This work is supported by a grant from the National Science Foundation, CHE-8117519. K.S.P. acknowledges support from the Henry and Camille Dreyfus Foundation for a teacher-scholar grant and the Alfred P. Sloan Foundation. L.E.M. thanks Dr. Dennis E. Vogel for helpful discussions during the early stages of this research.

Registry No. Ia, 1439-07-2; Ib, 1689-71-0; IIa, 93041-28-2; IIb, 93041-29-3.

---

(14) Cataliotti, R.; Paliani, G.; Sorriso, S.; Macchai, B.; Macchai, F. *Z. Phys. Chem. (Frankfurt am Main)* **1977**, *105*, 1.

Theoretical Study of Phosphate Interaction with NH_4^+, with Na^+, and with Mg^{2+} in the Presence of Water

C. V. Prasad and George R. Pack*

Contribution from the Department of Biomedical Sciences, University of Illinois College of Medicine at Rockford, Rockford, Illinois 61107. Received December 5, 1983

Abstract: The interactions of the phosphate anion with ammonium, sodium, and magnesium cations are studied by ab initio molecular orbital theory. Regions of the potential energy surfaces for anion–cation complex formation with two water molecules present are investigated. The theory predicts that the most stable structures for the monocation complexes have the water molecules partially between the anion and the cation. These bridging water molecules increase the separation distance between the ionic species in order to optimize the water–ion interactions. The addition of two water molecules is not predicted to affect the geometry of the magnesium phosphate complex. Implications for the association of cations with nucleic acids are discussed.

Introduction

The structure, function, and physical properties of nucleic acids are, to a large extent, determined by their polyanionic nature. The electrostatic repulsion resulting from the proximity of many negatively charged phosphate groups imposes severe constraints on the conformation of these polyions. In addition, the interaction of nucleic acids with regulatory proteins, drugs, or other molecules is affected by the very high charge density on the surface of the nucleic acid. The stability of these macroions is maintained by the association of small cations that are attracted to the very negative electrostatic potential near the nucleic acid surface. These counterions shield the phosphate–phosphate repulsions, affecting the intrapolymer energy and the stability of various conformations of DNA. In this way changes in the ionic environment can induce sequence-specific conformation changes in DNA.[1]

The nature of the DNA–cation interaction still remains unresolved. The formation of a "Stern layer"[2] on the immediate surface of the polyion may result from phosphate–cation ion-pair formation. Although simple phosphate–cation salts would be

---

(1) Pack, G. R.; Loew, G. *Biochim. Biophys. Acta* **1978**, *519*, 163–172.
(2) Schellman, J. A.; Stigter, D. *Biopolymers* **1977**, *16*, 1415–1434.

0002-7863/84/1506-8079$01.50/0 © 1984 American Chemical Society

Table I

system[a]	geometrical parameter	3-21G	extended basis set	binding energy[b]	
				3-21G	extended basis set
$(H_2O)_2$	$r(O\cdots O)$	2.81 Å	2.83 Å	−5.7	−5.1[c]
				(−9.5)	
$H_2PO_4^-\cdot H_2O$ (bifurcated)[f]	$r(O\cdots H)$	2.00 Å	2.07 Å	−16.1	−18.0[d]
				(−25.1)	(−22.5)[d]
$H_2PO_4^-\cdot H_2O$ (linear)[g]	$r(O\cdots H)$	1.65 Å	1.66 Å	−17.5	−20.1[d]
				(−22.9)	(−20.7)[d]
$H_2PO_4^-\cdot Na^+$	∠OPO	108.0°	110.0°	−125.8	−138.2[e]
	$r(P\cdots Na^+)$	2.68 Å	2.70 Å	(−154.8)	
$H_2PO_4^-\cdot Li^+$	∠OPO	104.6°	107.0°	−180.4	−162.5[e]
	$r(P\cdots Li^+)$	2.36 Å	2.29 Å	(−185.4)	
$H_2PO_4^-\cdot Mg^{2+}$	∠OPO	98.4°	102.0°	−361.3	−359.5[e]
	$r(P\cdots Mg^{2+})$	2.52 Å	2.43 Å	(−379.2)	

[a] All the systems have C_{2v} symmetry except $(H_2O)_2$. [b] The number in parentheses is the binding energy obtained without the BSSE counterpoise correction. [c] [541/31], ref 17. [d] 4-31G basis set. [e] Double ζ plus polarization basis set, ref 18. [f] Hydrogen bond between two anionic oxygens of the phosphate with the two hydrogens of water molecule. Geometry same as ref 13. [g] Hydrogen bond between one anionic oxygen and one of the hydrogen of water molecule (see ref 13).

highly dissociated in aqueous solution, the very high concentration of cations present at the polyion surface[3] increases the probability of such specific and direct interaction. Such a mode of binding implies that the cation is trapped in a relatively deep minimum on the potential energy surface for the phosphate–cation–water system. If a deep, localized, minimum does not exist, a more diffuse atmosphere of mobile cations, largely constrained to the immediate vicinity of the macroion, will predominate. If the small counterions are blocked by water molecules from forming close ion pairs with individual phosphate groups, all of the associated cations may be expected to be mobile within the electric double layer.

The mobile mode of binding involves a very large volume, and its theoretical evaluation requires a large number of interacting species. For this reason, statistical mechanical methods such as Monte Carlo simulations,[4] condensation theory,[5] Poisson–Boltzmann theory,[3,6] and molecular dynamics methods[7] have been used to study this association. Quantum-mechanical ab initio SCF methods have also been applied by various workers to study the geometry and electronic structure of site-bound complexes of phosphate–cations and their hydrated molecular systems.[8] We report here further ab initio molecular orbital theoretical calculations on the phosphate–cation–water system.

The present calculations are designed to give some insight into the degree to which site binding is preferred when ammonium, sodium, and magnesium separately bind to the phosphate anion in the presence of two water molecules. A portion of the potential energy surface for each of these complexes is examined in detail, and the results are discussed in the light of the two models of binding[5,9] that may exist for such systems.

Methods

The GAUSSIAN 80 program obtained from QCPE[10] was used for the calculations reported here. The basis set used was the split-valence (3-21G) basis set, which has been shown to yield good equilibrium geometries when tested on a number of small molecules.[11] The reliability of this basis set for the calculation of equilibrium geometries of molecular complexes of the type of interest to this study has been addressed here by comparison with results obtained using larger basis sets.

It is well known that the use of truncated basis sets gives rise to basis set superposition errors (BSSE) when applied to the study of intermolecular interactions. The counterpoise correction[12] may be applied to reduce the error in calculated interaction energies. This is done by defining the interaction energy to be

$$\Delta E_{AB} = E_{AB} - E_A - E_B$$

where E_{AB} is the total energy of the molecular complex AB; E_A and E_B are the energies of the subsystems A and B, calculated using the full basis set of the complex. This correction has been applied to all of the minimum energy geometries calculated by the 3-21G basis set that are reported in the present paper.

We have attempted to assess the reliability of the 3-21G basis set for the prediction of equilibrium geometries and energies by comparing the results with those from larger basis sets. The comparison is summarized in Table I. Alagona et al.[13] have reported calculations, using the 4-31G basis set, on the $H_2PO_4^-\cdot H_2O$ complex. They noted that, in contrast to the minimal basis set STO-3G, the 4-31G calculations predict a "bifurcated" hydrogen-bond geometry to be more stable than the "linearly" hydrogen-bonded geometry for this complex. We have repeated these calculations at both the 4-31G and the 3-21G levels. Uncorrected SCF calculations using both basis sets predict the bifurcated geometry to be more stable than the linear by 1.7 and 2.2 kcal/mol, respectively. When the correction for BSSE is applied to these calculations, there is a remarkable reversal in the orders of stabilities calculated by both 4-31G and by 3-21G. The linear structure is calculated to be favored by 2.1 and 1.2 kcal/mol using the 4-31G and the 3-21G basis sets, respectively. This reversal in the depth of the local minima demonstrates the need of the correction for BSSE even at the 4-31G level. This is particularly evident in the present case where the correction is large for the bifurcated geometry and small for the linear structure. We find that the linear water dimer, as calculated by the 3-21G basis, has a hydrogen-bond distance of 2.81 Å, very similar to that given by 4-31G,[14] although still a bit short of the experimental distance of 2.98 Å.[15] Although the uncorrected 3-21G energy

---

(3) Klein, B. J.; Pack, G. R. *Biopolymers* **1983**, *22*, 2331–2352.

(4) Clementi, E.; Corongiu, G. *Biopolymers* **1982**, *21*, 763–777.

(5) Manning, G. S. *Q. Rev. Biophys.* **1978**, *11*, 179–246.

(6) (a) Gueron, M.; Wiesbuch, G. *Biopolymers* **1980**, *19*, 353–382. (b) Stigter, D. *J. Colloid Interface Sci.* **1975**, *53*, 296–306.

(7) (a) Perez, P.; Prohofsky, E. W. *J. Chem. Phys.* **1984**, *80*, 3785–3790. (b) Lee, W. K.; Prohofsky, E. W. *Ibid.* **1981**, *75*, 3040–3052, and references therein.

(8) (a) Pullman, A.; Berthod, H.; Gresh, N. *Int. J. Quant. Chem. Symp.* **1976**, *10*, 59–76. (b) Gresh, N.; Pullman, B. *Theor. Chim. Acta* **1979**, *52*, 67–73. (c) Pullman, B.; Pullman, A.; Berthod, H. *Int. J. Quant. Chem. Quantum Biol. Symp.* **1978**, *5*, 79–90. (d) Berthod, H.; Pullman, A. *Chem. Phys. Lett.* **1977**, *46*, 249–252. (e) Marynick, D. S.; Shaefer, H. F. *Proc. Natl. Acad. Sci. U.S.A.* **1975**, *73*, 3794–3798. (f) Pullman, A.; Berthod, H. *Chem. Phys. Lett.* **1976**, *41*, 205–209.

(9) Clement, R. M.; Sturm, J.; Daune, M. P. *Biopolymers* **1973**, *12*, 405–421.

(10) van Kampen, P. N.; deLeew, F. A. A. M.; Smits, G. F.; Altona, C. QCPE Program 437 GAUSSIAN 80: IBM version (a translation of QCPE 406 by Pople et al.)

(11) Binkley, J. S.; Pople, J. A.; Hehre, W. J. *J. Am. Chem. Soc.* **1980**, *102*, 939–947.

(12) Boys, S. F.; Bernardi, F. *Mol. Phys.* **1970**, *19*, 553–566.

(13) Alagona, G.; Ghio, C.; Kollman, P. A. *J. Am. Chem. Soc.* **1983**, *105*, 5226–5230.

(14) Dill, J. D.; Allen, L. C.; Topp, W. C.; Pople, J. A. *J. Am. Chem. Soc.* **1975**, *97*, 7220–7226.

(15) Dyke, T. R.; Muenter, J. S. *J. Chem. Phys.* **1974**, *60*, 2929–2930.

Table II

system[a]	geometrical parameter[b]		energy (kcal/mol)
H_2O	∠HOH[c]	104.5	-47 431.4
	r(OH)[c]	0.96	
NH_4^+	r(NH)	1.02	-35 287.8
	∠HNH[c]	109.5	
$H_2PO_4^-$ (I)	∠O1PO2[c]	101.8	-400 336.1
	∠O3PO4[c]	115.5	
	POH[c]	119.0	
$H_2PO_4^-$	O1PO2	95.1	-400 339.2
	∠O3PO4	119.9	

[a] All the molecules are in C_{2v} point group, except NH_4^+ (D_{2d}). [b] Angles in degrees and lengths in ångstroms. [c] These parameters were not optimized.

is -9.7 kcal/mol, when these calculations are corrected for BSSE, 3-21G yields a binding energy of -5.7 kcal/mol, which is remarkably close to the experimentally estimated value[16] of -5.2 ± 1.5 and to the HF energy of -5.1 kcal/mol.[17]

A comparison shown in Table I of the equilibrium geometries of the $H_2PO_4^-$ complexes with Na^+, Li^+, and Mg^{2+}, calculated by 3-21G with those calculated using an optimized double ζ plus polarization basis set,[18] again suggests that 3-21G yields results that may be taken as reliable. These calculations, in which the OPO angle and the metal–phosphorus atom distance were relaxed, show less than 0.1 Å difference in the metal–phosphorus distance and only a few degrees difference in the OPO angles. It might be noted that STO-3G[8e] has predicted significantly different angles and distances for these complexes. BSSE corrected binding energies of the 3-21G basis set compare well with the extended basis set results (the last two columns of Table I), allowing for a more confident interpretation of the interaction energies. It will also be noted, while examining the potential energy surfaces for phosphate–cation–water complexes, that the shape and general position of minima (Figures 1 and 2) do not change upon correction for superposition error. The 3-21G basis set, therefore, seems remarkably reliable for the calculation of the qualitative structures of the molecular complexes involving phosphate anion, water, and small metal cations. When corrected for BSSE, the binding energies are also in agreement with the results of larger calculations. This allows the application of this somewhat small basis set to a somewhat larger system. In this way a reliable search of the potential energy surface for ion-pair formation in the presence of two water molecules is made possible.

Results

Energies of the isolated molecules $H_2PO_4^-$, NH_4^+, and H_2O were computed first. For the H_2O molecule, no internal geometry optimization was done. An HOH bond angle of 104.5° was used and the OH bond length was 0.96 Å. The energy of the NH_4^+ cation was computed optimizing only the NH bond lengths. In the case of $H_2PO_4^-$ (I), the energies were calculated for the geometry that the phosphate group assumes in the B form of DNA,[19] with the hydrogen atoms placed to retain C_{2v} symmetry.

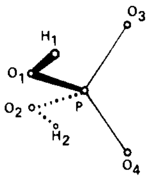

I

Table III

system[a]	geometrical parameter[b]		energy (kcal/mol)	interaction energy (kcal/mol)[c]
	Complex II			
$H_2PO_4^- \cdot NH_4^+$ (II)	∠O1PO2	96.3	-435 741.0	-115.3
	∠O3PO4	111.1		
	r(O···H)	2.28		
	r(N···P)	3.16		
	r(N–H)	1.01		
	Complex III			
$H_2PO_4^- \cdot NH_4^+$	∠O1PO2	97.2	-435 766.7	-139.7
	∠O3PO4	112.5		
	r(O···H)	1.63		
	r(N··P)	3.02		
	r(N–H)	1.06		
$H_2PO_4^- \cdot NH_4^+$	∠O1PO2[d,e]	95.1	-435 763.4	-136.4
	∠O3PO4[d,e]	119.9		
	r(O···H)	1.65		
	r(N···P)	2.96		
	r(N–H)	1.06		
$H_2PO_4^- \cdot NH_4^+$	∠O1PO2[d,f]	101.8	-435 765.4	-138.7
	∠O3PO4[d,f]	115.5		
	r(O···H)	1.64		
	r(N···P)	2.99		
	r(N–H)	1.06		
$H_2PO_4^- \cdot NH_4^+$	∠O1PO2[d,f]	101.8	-435 764.0	-137.0
	∠O3PO4[d,f]	115.5		
	r(O···H)	1.65		
	r(N···P)	3.00		
	r(N–H)[d,e]	1.02		

[a] All the complexes are in C_{2v} point group. [b] Angles in degrees and lengths in ångstroms. [c] $E_{\text{interaction}} = E(H_2PO_4^-) + E(NH_4^+) - E_{\text{complex}}$. BSSE correction was not applied to these calculated energies. [d] These parameters were not optimized. [e] Values from isolated molecule optimization. [f] Experimental values.[19]

Calculations were also done in which the O1–P–O2 and O3–P–O4 bond angles were allowed to relax. The optimized angles are 95.1 and 119.9°, respectively. This optimization lowers the energy of the anion by 3.1 kcal/mol (Table II).

Ammonium. Gresh and Pullman[8b] have examined the principal modes of binding of the ammonium cation to phosphate and found that a geometry in which the ammonium ion symmetrically interacts with the phosphate anionic oxygens is the most stable. In order to study the possibilities of ion-pair formation for this system in the presence of water molecules, we investigated two geometries. Complex II has NH_4^+ binding to $H_2PO_4^-$ symmetrically through the H3 and H4 hydrogens, forming bifurcated hydrogen bonds with the anionic oxygens O3 and O4, such that the H3–N–H4 plane is perpendicular to the O3–P–O4 plane. Complex III differs from II in that the NH_4^+ is rotated by 90° about the C_2 symmetry axis, such that the H3–N–H4 and O3–P–O4 planes coincide. The hydrogen bonds in this arrangement are pseudo-linear rather than bifurcated. The O1–P–O2 and O3–P–O4 bond angles, the N–P distance, and the H3–N and H4–N bond lengths were relaxed in the calculations of the geometry. Comparison of the total complex energies indicates that the optimized complex III is more stable than the optimized bifurcated complex II by a rather significant 24.4 kcal/mol (Table III). This result is in agreement with Gresh and Pullman's work.[8b] This clearly is the result of

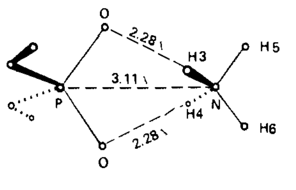

II

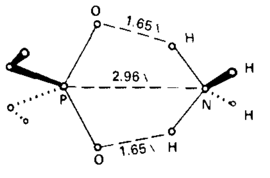

III

---

(16) Gebbie, H. A.; Borroughs, W. J.; Chamberlain, J.; Harris, J. E.; Jones, R. G. *Nature (London)* **1969**, *221*, 143–145.

(17) Diercksen, G. H. F.; Kraemer, W. P.; Roose, B. O. *Theor. Chim. Acta* **1975**, *36*, 249–274.

(18) Liebmann, P.; Loew, G.; McLean, A. D.; Pack, G. R. *J. Am. Chem. Soc.* **1982**, *104*, 691–697.

(19) Arnott, S.; Hukins, D. W. L. *Biochem. Biophys. Res. Commun.* **1972**, *47*, 1504–1509.

Table IV

system[a]	geometrical parameters[b]		energy (kcal/mol)	interaction energy (kcal/mol)[c]
$H_2PO_4^-NH_4^+\cdot H_2O$	r(N···P)	2.9	−483 206.0	−135.8[d]
(IV)	r(O···H)	1.69		(−147.7)[e]
	r(N···O(W))	2.81		
$H_2PO_4^-NH_4^+\cdot H_2O$	r(N···P)	5.5	−483 175.7	−102.9
(V)	r(O···H)	1.78		(−117.4)
	r(P···O(W))	3.03		
$H_2PO_4^-NH_4^+\cdot H_2O$	r(N···P)	3.05	−683 209.2	−139.8
(VI)	r(O···H(W))	1.80		(−150.9)
	r(O···H(N))			
$H_2PO_4^-NH_4^+\cdot 2H_2O$	r(N···P)	3.05	−530 655.4	−129.9
(VII)	r(O···H)	1.75		(−165.6)
	r(O(W)···H)	1.8		
$H_2PO_4^-NH_4^+\cdot 2H_2O$	r(N···P)	4.75	−530 681.2	−170.0
(VIII)	r(O···H)	1.5		(−191.4)
	r(H-O(W)···H)	1.5		
$H_2PO_4^-Na^+\cdot 2H_2O$	r(Na$^+$···P)	2.76	−596 234.4	−161.7
(XIV)	r(Na$^+$···O(W))	2.17		(−206.5)
	∠O3PO4	110.4		
$H_2PO_4^-Na^+\cdot 2H_2O$	r(Na$^+$···P)	3.12	−596 251.2	−172.9
(XV)	r(Na$^+$···O(W))	2.11		(−223.9)
	∠O3PO4	111.0		
$H_2PO_4^-Na^+\cdot 2H_2O$	r(P···O(WI))		−596 213.2	−138.5
(XVI)	r(O(W)···Na$^+$)			(−185.3)
	r(Na$^+$···O(W2))			
$H_2PO_4^-Mg^{2+}\cdot 2H_2O$	r(Mg^{2+}···P)	2.58	−619 768.8	−491.7
(XIX)	r(Mg^{2+}···O(W))	1.94		(−513.7)
	∠O3PO4	100.3		

[a] All the complexes in C_{2v} point group, except VI which has C_s point group. [b] Angles in degrees and lengths in ångstroms. [c] $E_{\text{interaction}} = E(M^+) + E(H_2O) + E(H_2O) + E(H_2PO_4^-) - E_{\text{complex}}$. $M^+ = NH_4^+, Na^+, Mg^{2+}$. [d] $E_{\text{interaction}} = E(NH_4^+) - E(H_2O) - E(H_2PO_4^-) - E_{\text{complex}}$. [e] Number in parentheses is the interaction energy obtained with 3-21g basis set without the BSSE correction.

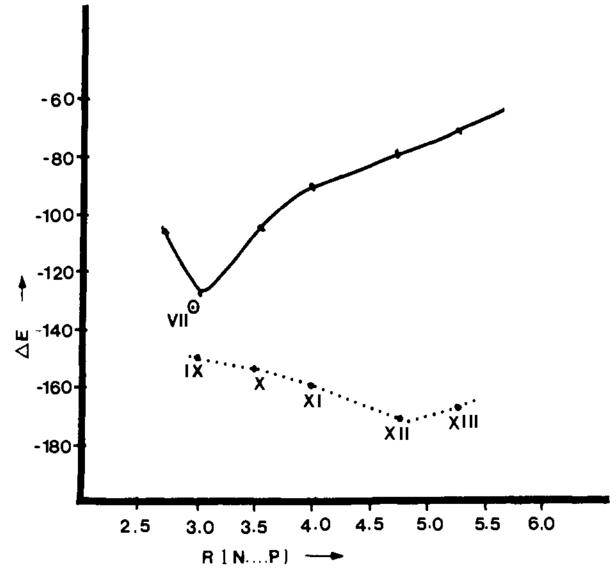

Figure 1.

the formation of shorter, linear hydrogen bonds, as shown in III, compared to the bifurcated hydrogen bonds shown in II.

To study the effect of geometry optimization on the calculated equilibrium geometries, the following calculations were done, starting from the stable $H_2PO_4^-\cdot NH_4^+$ complex III. First, the $H_2PO_4^-$ geometry was kept frozen at the experimental[19] geometry, while optimizing the nitrogen–phosphorus distance as well as the H3–N and H4–N bond lengths. In the second set of calculations, the $H_2PO_4^-$ was frozen in the geometry that had been obtained by optimizing the O1–P–O2 and O3–P–O4 bond angles of the isolated anion, described above. The nitrogen–phosphorus distance and the H3–N and H4–N bond lengths were again optimized. A third set of calculations was done freezing the geometries of both interacting species and optimizing only the nitrogen–phosphorus distance along the C_2 axis. It can be seen from Table III that relaxation of the internal geometries of the molecules does not significantly affect the equilibrium geometries of the complex. The NH bond-length variation has no appreciable effect. The optimized geometry for the complex does not vary significantly even for a large change in O3–P–O4 bond angle. Hence, in the further calculations involving the $H_2PO_4^-\cdot NH_4^+$ complex, the internal geometries of the interacting species were kept at the values obtained from the optimization of the isolated molecules.

A reaction coordinate analysis for the $H_2PO_4^-\cdot NH_4^+$ complex at various N–P distances was carried out, retaining the C_{2v} symmetry of the complex. Energies obtained at nitrogen–phosphorus distances of 2.68, 3.00, 3.55, 4.00, 4.75, and 5.26 Å, as well as the minimum 2.96 Å, were plotted, and the potential energy curve is shown in Figure 1. The steepness of this curve is typical of in vacuo potentials for ionic interactions.

The effect of adding a single water molecule to the $H_2PO_4^-\cdot NH_4^+$ complex was investigated by exploring different regions of the potential energy hypersurface. In the first, a water molecule was placed "outside" the $H_2PO_4^-\cdot NH_4^+$ complex (IV), with the HOH angle bisected by the C_2 axis of the complex. In the second, the water molecule was interposed between the $H_2PO_4^-$ and NH_4^+, forming a complex with a geometry as indicated in V. In the first two of these cases, the nitrogen–phosphorus distance and the

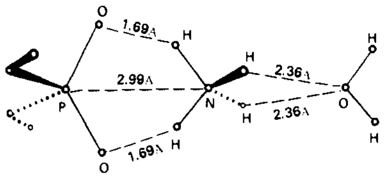

IV

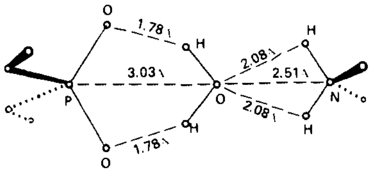

V

Table V. Gross Atomic Charges for the Stable Ionic Complexes (3-21G)

system/atom	P	O1	O3	H1	$H_2PO_4^-$	N	H3	H4	NH_4^+	M^+	O	H1	H2	H_2O
I. $H_2PO_4^-$	1.96	-0.90	-0.97	0.39	-1.0									
III. $H_2PO_4^-{\cdot}NH_4^+$	2.06	-0.87	-0.96	0.41	-0.78	-0.98	0.49	0.39	0.78					
IV. $H_2PO_4^-{\cdot}NH_4^+{\cdot}H_2O$	2.06	-0.87	-0.96	0.41	-0.78	-0.98	0.67	0.39	0.75		-0.75	0.39	0.39	0.03
VIII. $H_2PO_4^-NH_4^+{\cdot}2H_2O$	2.09	-0.87	-0.97	0.41	-0.77	-1.06	0.50	0.39	0.72		-0.85	0.50	0.39	0.04
VII. $H_2PO_4^-{\cdot}NH_4^+{\cdot}2H_2O$	2.04	-0.87	-0.95	0.41	-0.81	-1.07	0.46	0.42	0.69		-0.73	0.40	0.39	0.06
XV. $H_2PO_4^-{\cdot}Na^+{\cdot}2H_2O$	2.16	-0.87	-0.99	0.43	-0.70					0.58	-0.82	0.40	0.48	0.06
XX. $H_2PO_4^-{\cdot}Mg^{2+}{\cdot}2H_2O$	2.20	-0.82	-0.98	0.45	-0.50					1.18	-0.81	0.48	0.49	0.16

nitrogen–water oxygen distances were optimized, maintaining the C_{2v} complex symmetry and the rigid geometries of the interacting species. A third geometry was also investigated. The water molecule was positioned in such a way that it interacted with both the anion and the cation, forming hydrogen bonds with both of the ions. The equilibrium geometry for this system was obtained by allowing the water molecule to freely move in the O3–P–O4 plane. The optimal geometry found is shown as complex VI.

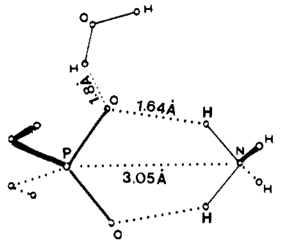

VI

When the interaction energies for these complexes are compared (see Table IV), it is clearly seen that exact interposition of a water molecule between the two ions (complex V) is not at all preferred (Table IV). On the other hand, it seems possible to have low-energy modes of binding when the water is outside (complex IV) or partially hydrogen bonded to one of the ions (complex VI).

Next, the problem of adding two water molecules to the $H_2PO_4^-{\cdot}NH_4^+$ complex was addressed. The results presented in Table IV indicate that when one water molecule is added to the $H_2PO_4^-{\cdot}NH_4^+$ complex, it is energetically unfavorable that the water will directly come between the ions. However, when two water molecules are added, it is possible to have low-energy modes of binding in which the waters are neither directly between nor completely external to the ion pair, but rather are directly interacting with both species while minimally blocking the anion–cation interaction. In order to compare the stabilities of the various binding modes, different regions of the potential surface were again compared. In the first series of calculations on this system, the two water molecules were placed "outside" of the $H_2PO_4^-{\cdot}NH_4^+$ complex, such that water oxygens face the hydrogen atoms H5 and H6 of the NH_4^+, which were oriented away from the anion. The nitrogen–phosphorus distance and the nitrogen–water oxygen distances were varied, maintaining the C_{2v} symmetry of the entire complex. The equilibrium geometry is that shown in VII.

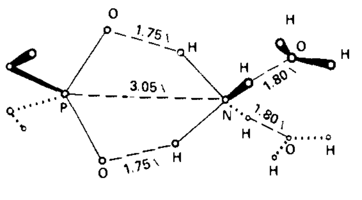

VII

The portion of the energy surface corresponding to two water molecules in-between the $H_2PO_4^-$ and the NH_4^+ was investigated in detail. This geometrical arrangement (VIII) has each water molecule forming two hydrogen bonds, thus acting as a bridge between the anion and the cation. The orientation of each of these water molecules was optimized by varying the N–H···OW angles, the N–H···OW distances and the H···O–HW angle, allowing complete orientational freedom in the O3–P–O4 plane for both of the water molecules. In addition to these parameters, the N–P distance was also varied. Structure VIII shows the equilibrium geometry obtained after this optimization. It should be noted that two water molecules have increased the N···P distance from 2.96 (complex III) to 4.75 Å (complex VIII). This 4.75-Å separation is still short of the 5.54-Å N···P distance that is required for a water molecule to actually fit between the ions, as in complex V.

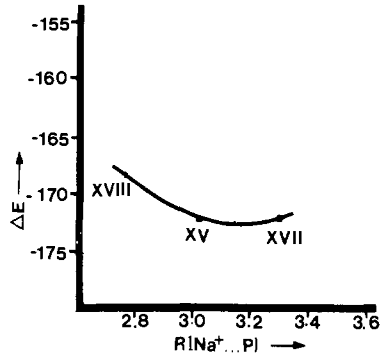

Figure 2.

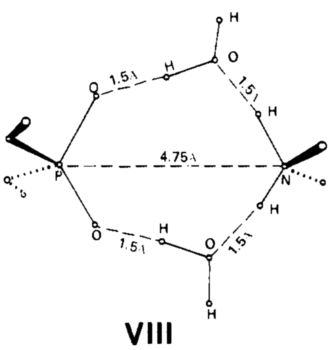

VIII

A reaction coordinate analysis was carried out with the N–P distance along the C_2 axis as the variable (structures IX through XIII). In these calculations, the water molecules were allowed to orient to their minimum energy positions within the O3–P–Op4 plane. A plot of energy vs. distance obtained in this analysis is shown in Figure 1. Complex IX shows the optimal positioning of the water molecules about a complex which has essentially the optimal in vacuo geometry of complex III. Although the anion–cation interaction is optimal here, the hydrogen bonding between the ammonium and the water is very highly strained. As the ammonium separates from the phosphate (IX through XII), the energy progressively decreases as the waters orient to optimize their hydrogen bonding. The minimum (XI) is reached when water molecules can form two linear hydrogen bonds with O···O and O···N distances of about 2.5 Å. This hydrogen-bond distance is slightly less than the 2.61 Å that the 3-21G basis set predicts for the linear $H_2PO_4^-{\cdot}H_2O$ complex (Table I), as a result of the electron withdrawal by the NH_4^+. As the ammonium ion separates farther from the phosphate, as in complex XIII, the energy increases. In solution, more water molecules would be available to decrease this effect. Therefore, the calculations lose relevance shortly beyond the minimum energy position. The theory does indicate, however, that even as few as two water molecules can keep the N···P distance from decreasing beyond 4.75 Å. It also

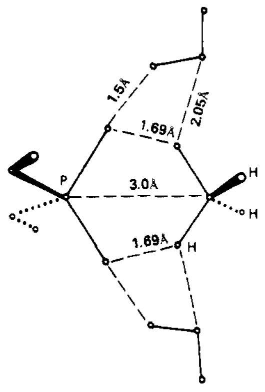

IX

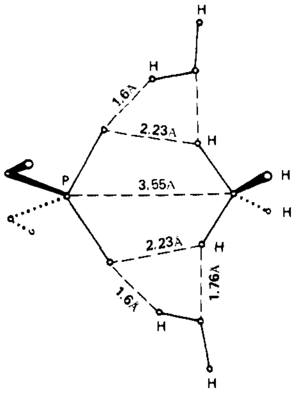

X

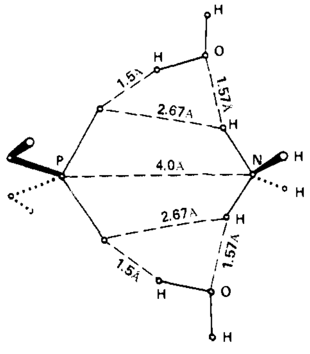

XI

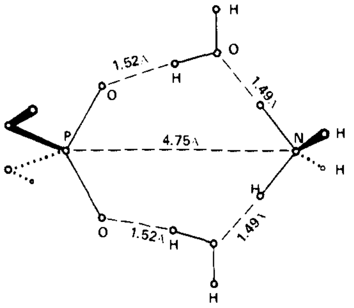

XII

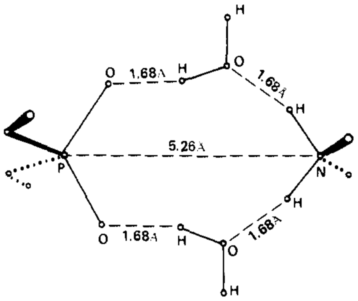

XIII

should be noted that complex VII, in which the two water molecules are "outside" of the ion pair, is 40.1 kcal/mol higher in energy than is complex VIII (or XII), as is shown in Table IV.

Sodium. Equilibrium geometries of the $H_2PO_4^-\cdot Na^+\cdot 2H_2O$ complexes were also investigated. The water molecules were placed in three qualitatively different orientations. The first two correspond to the two minima VI and VII found for the NH_4^+ case. In complex XIV, the interacting species were placed with the water oxygen constrained to a line that bisects the HOH angle and intersects the C_2 axis at the metal ion, subtending an angle of 109.5°. The energies were computed optimizing the metal cation–water oxygen distance, as well as the position of the metal ion along the C_2 axis. In addition to these geometric parameters, all of which were relaxed in the study of the NH_4^+ complexation, the O3–P–O4 angle was allowed to vary in these calculations on the Na^+ complex. This variable was introduced because previous studies[18] have shown that this angle changes significantly when phosphate complexes with different metal cations, a result confirmed at the 3-21G level by the present work.

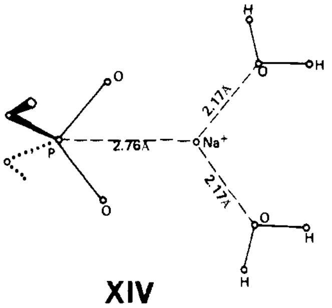

XIV

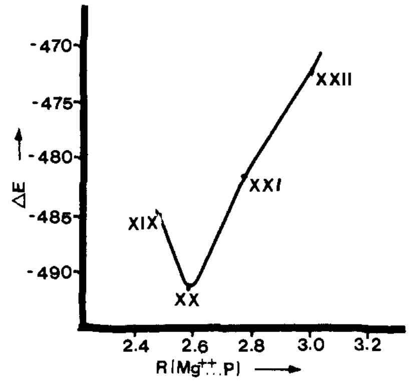

Figure 3.

The second orientation of the water molecules investigated is similar to the stable $H_2PO_4^-\cdot NH_4^+\cdot 2H_2O$ geometry, VIII. The minimum energy geometry is depicted in structure XV. The orientation of the water molecules was optimized by varying the Na–water oxygen distance, the Na–O–H bond angle, and the P–Na–O angle. In addition, the Na–P distance and the O3–P–O4 angle were varied. Table IV shows that this geometry is preferred over the geometry in which the water molecules are constrained to be "outside" (i.e., XV is 11.2 kcal/mol more stable than XIV). This difference represents the greater freedom of the water molecules in XV. When the P–Na–O and Na–O–H angles are allowed to vary, conferring to the water freedom of orientation in the O3–P–O4 plane, structure XIV relaxes directly to structure XV, clearly showing the preference for the bridging effect of the water.

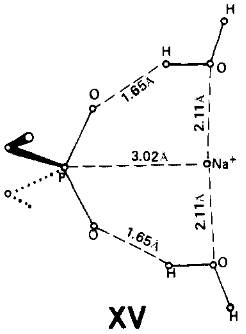

XV

The third distinct geometry considered was a C_{2v} structure in which the water molecules are positioned on either side of the sodium ion with one water forming hydrogen bonds with the phosphate anion (complex XVI). The optimal geometry was obtained by relaxing the various ion–water oxygen distances, viz., P-OW(1), OW(1)-Na^+, and Na^+-OW(2) along the C_2 axis (complex XVI). However, the interaction energy of this complex is 31.2 kcal/mol higher than that of complex XV, once again showing the preference for bridged arrangement of water molecules for this system (Table IV).

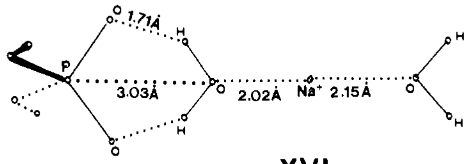

XVI

Reaction coordinate analysis for Na^+ was carried out with the phosphorus–metal ion distance as the variable, optimizing the orientation of the water molecules in the O3–P–O4 plane as well as the O3–P–O4 angle. Energies obtained at various positions of the Na^+ along the C_2 axis are plotted in Figure 2. Structures XVII and XVIII represent points on this curve on either side of the minimum represented by XV. The Na^+ ion approaches the phosphate group much closer than does the center of the ammonium ion under similar conditions, as a comparison of the minima XV and VIII illustrates. Although the water molecules are oriented similarly in both complexes, there are notable differences, stemming primarily from the possibility of a bridging hydrogen bond network that stabilizes the NH_4^+ complex but is not possible in the Na^+ complex.

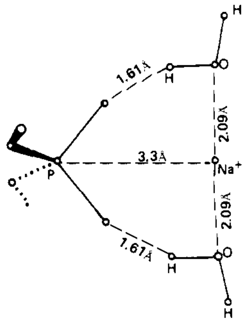

XVII

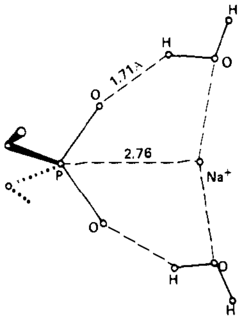

XVIII

Magnesium. In a similar vein, the interaction of Mg^{2+} with $H_2PO_4^-$ in the presence of two water molecules was studied. The equilibrium geometry for this complex was investigated, allowing the waters to relax in the O3–P–O4 plane, varying the O3–P–O4 angle for different positions of the Mg^{2+} along the C_2 axis. Structures XIX through XXII depict the movement of water molecules for four different values of the divalent cation to phosphate distance. The minimum occurs when the phosphorus-to-Mg^{2+} distance is also allowed to vary as given in XX. The energies of these structures are plotted in Figure 3.

Table V shows the gross atomic charges and the extent of charge transfer for the stable molecular complexes investigated.

Discussion

The results from the study of the ammonium ion interacting with the phosphate group, without any water molecules present, show the formation of strong hydrogen bonds, resulting in a very deep minimum on the potential energy surface (solid line, Figure 1). The addition of a single water molecule to this complex shows that two low-energy modes of binding are possible. When the water is external to the ion pair, the geometry of the ion pair remains unaltered (compare III with IV). In another orientation (complex VI), the water molecule can partially interact with one of the ions forming hydrogen bonds, and the interaction between the anion and the cation remains direct. However, interposition of the water molecule directly between the two ions would only lead to a less stable structure. This result can be interpreted as indicating that a single water molecule cannot separate the ions of an ion pair formed by NH_4^+ and phosphate.

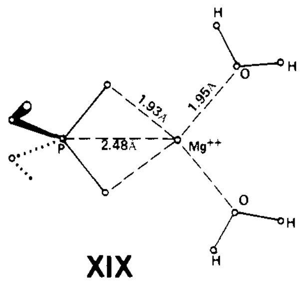

XIX

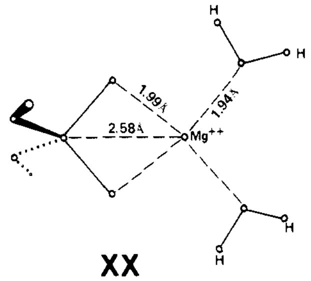

XX

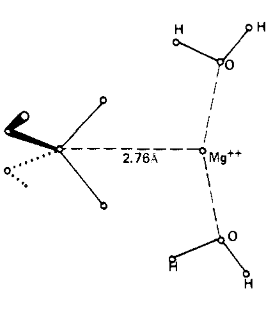

XXI

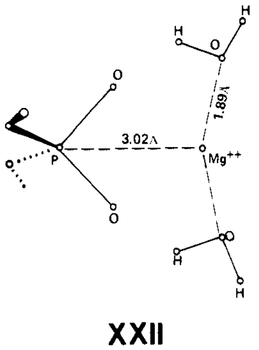

XXII

Even at the very high concentrations of cation attracted to the vicinity of a polyanion such as DNA, there is likely to be more than a single water molecule available for ionic hydration. The calculations that were done on the ammonium phosphate complex in the presence of two water molecules suggest that as few as two waters can significantly alter the most probable geometry of the complex. The most favored complex (VIII) has a stable geometrical arrangement in which the two waters form a bridge between the ions. This geometry, in which both of the ions are hydrated by the same water molecules, results in a shift in the minimum of the potential curve. Figure 1 shows that the distance of approach of ammonium to the phosphate group increases by about 1.75 Å on the addition of two waters. This increase is not great enough to allow a water molecule to fit directly between the ions, yet it prevents the direct hydrogen-bond formation between the ions that is seen when less than two waters are present. The two curves in Figure 1 are the interaction energies for the $NH_4^+ \cdot H_2PO_4^-$ and for the four molecule system $H_2PO_4^- \cdot NH_4^+ \cdot 2H_2O$. The minima are quite distinct, showing the interaction of the hydrated complex being stronger than the unhydrated one. This points to the probability of a unique structure of ion pairs in the presence of two water molecules. The positions that the water molecules assume as the ion–ion distance increases, shown in structures IX through XIII, indicate that the waters push the ions apart in order to maximize their hydrogen bonding with both ions. Structure VII, in which the waters do not directly interact with the anion, is significantly higher in energy.

The interaction of phosphate with Na^+ is in some ways very similar to its interaction with NH_4^+, particularly in the presence of two water molecules. The series of structures XV, XVII, XVIII, calculated allowing relaxation of H_2O positions, indicates that the water molecules again interact with both ionic species. The minimum-energy structure, XV, in which the P to Na^+ distance is 3.02 Å, shows an increase in the ion–ion distance over the 2.68-Å minimum that is found for the complex without water (Table I). Perhaps the most notable feature of the potential energy curve for this complex with two waters (Figure 2) is its flatness. This lack of a distinct, deep minimum appears to indicate that when Na^+ binds to DNA it remains nonlocalized, creating a counterion atmosphere around the polyion and suggests that direct site binding may be of little importance in this case.

In contrast to the complexes that phosphate forms with the monocations studied, the phosphate–Mg^{2+} interaction is direct, with sufficient energy such that the addition of two water molecules cannot effectively cause a modification of the ion-pair geometry. Structures XIX through XXII indicate that the optimal position for the water molecules is one in which there is minimal interference in the interaction between the ions. The close approach of Mg^{2+} to the phosphorus atom is not markedly altered by two waters, although these waters optimize their positions to allow maximum interionic interactions. The steepness of the potential curve in Figure 3 is consistent with ion-pair formation in solution, although these calculations with only two water molecules cannot definitively argue for site binding of Mg^{2+} in solution. However, recent experimental evidence does suggest that Mg^{2+} directly site binds to the phosphate groups of DNA in solution.[20]

Conclusions

Several inferences regarding the possibility of the formation of ion pairs between phosphate and the small cations present in the very high concentrations at nucleic acid surfaces can be made. For the monovalent cations, NH_4^+ and Na^+, similar minima are found for the four molecule potential surface involving phosphate and two water molecules. These minima are distinctly different from the minima that occur with no water present. The effect of the water does not appear to be to solvate the optimal ion pair. Rather the water becomes an integral part of the complex, increasing the anion–cation distance but not disrupting the interaction completely. It seems clear from these calculations that neither NH_4^+ nor Na^+ would form a close contact ion pair with phosphate groups of the nucleic acid backbone. From the shape of the very flat potential (Figure 2) for the interaction of Na^+ with $H_2PO_4^-$ in the presence of two water molecules, it may be concluded that Na^+ would not even form a static hydrated complex of the type indicated by complex XV. Instead, the association of Na^+ with nucleic acids is expected to be completely as mobile ions moving in the highly electrostatic potential surrounding the polyanion.

The binding of Mg^{2+} is much stronger than that of the monovalent cations. The steepness of the potential shown in Figure 3 clearly shows that unlike the monovalent cations, Mg^{2+} cannot be displaced from its site-bound position by the addition of two water molecules. This is an indication that Mg^{2+} might interact by direct site binding, although calculations with only two water molecules are not sufficient to allow definitive statements in this regard.

Acknowledgment. This work was supported by Grant R01-GM29079 from the National Institute of General Medical Sciences. Additional generous support from the Sundstrand Corporation is gratefully acknowledged. We thank Dr. Gilda Loew for helpful discussions on various aspects of this problem.

---

[20] Taboury, J. A.; Bourtayre, P.; Ligier, J.; Taillandier, E. *Nucleic Acids Res.* **1984**, *12*, 4247–4258.

Cleft Formation upon Polymerization of Surfactant Vesicles

Faruk Nome,[1] Wayne Reed, Mario Politi, Pietro Tundo,[2] and Janos H. Fendler*

Contribution from the Department of Chemistry and Institute of Colloid and Surface Science, Clarkson University, Potsdam, New York 13676. Received June 1, 1984

Abstract: Morphological consequences of the photopolymerization of vesicles prepared from $(C_{18}H_{37})_2N^+(CH_3)CH_2C_6H_4$-*p*-$CH{=}CH_2,Cl^-$, **1**, have been investigated by using 8-hydroxy-1,3,6-pyrenetrisulfonate (POH) as a reporter group. Static and dynamic laser light scattering established the hydrodynamic radius and the molecular weight of **1** vesicles to be 425 ± 25 Å and 2.3×10^7. Neither of these values changed upon polymerization. POH was shown to bind appreciably to **1** vesicles. Excitation of POH, following immediately its addition to nonpolymerized **1** vesicles, resulted in fluorescence emission with maxima at 440 and 520 nm. Incubation led to time-dependent changes of this spectra. Increasing incubation time of POH containing nonpolymerized **1** vesicles resulted in the gradual disappearance of the emission band at 520 nm and in the concomitant increase of the emission band at 440 nm. Fluorescence spectra of POH did not show any time-dependent changes following its addition to polymerized **1** vesicles. These results were interpreted in terms of the gradual penetration of POH into nonpolymerized **1** vesicles and in terms of long-term stabilization of POH in the clefts formed on the vesicle surface upon pulling the surfactant head groups together by photopolymerization. Differences between nonpolymerized and polymerized vesicles also manifested in the excited state protonation equilibria

$$(\mathrm{POH})^* \underset{k_{\mathrm{on}}^*}{\overset{k_{\mathrm{off}}^*}{\rightleftharpoons}} (\mathrm{PO}^-)^* + \mathrm{H}^+$$

A k_{off}^* value of $4.3 \times 10^9\ \mathrm{s}^{-1}$ was obtained in nonpolymerized vesicles immediately after the POH injection. Following a day of incubation no excited-state proton ejection could be observed in nonpolymerized **1** vesicles. Consequently, a k_{off}^* value of $6.1 \times 10^9\ \mathrm{s}^{-1}$ was observed in nonpolymerized vesicles both immediately and 1 day subsequent to the addition of POH to polymerized **1** vesicles. Similar behavior has been observed for the steady-state (P) and nanosecond time-resolved polarizations, τ_R values, of POH, as well as that for the ground state PO^- reprotonation (governed by k_{on}) in nonpolymerized and polymerized **1** vesicles. In nonpolymerized **1** vesicles, P values increased (from 0.12 to 0.19), τ_R was determined to be ≥50 ns, and k_{on} values ($4 \times 10^8\ \mathrm{M}^{-1}\ \mathrm{s}^{-1}$) became unobservable after a day of incubation. In polymerized **1** vesicles, P values of 0.08, τ_R values of 4 ns, and k_{on} values of $8 \times 10^8\ \mathrm{M}^{-1}\ \mathrm{s}^{-1}$ remained unaffected by incubation.

The ever increasing utilization of organized surfactant aggregates in reactivity control, drug delivery, and photosensitized water splitting have necessitated the development of new systems.[3,4] Polymerized surfactant vesicles have become highly popular within a remarkably short time since polymerization has provided an unprecedented degree of stability and permeability control as well as opened the door to domain-controlled substrate release.[5-17]

---

[1] Permanent Address: Depto. de Quimica, Universidade Federal de Santa Catarina, 88000—Florianopolis, Santa Catarina, Brazil.

[2] Permanent Address: Istituto Di Chimica Organica, Della Universita de Torino, 10125 Torino, Via Bidone 36, Italy.

[3] Fendler, J. H. "Membrane Mimetic Chemistry"; Wiley-Interscience: New York, 1982.

[4] Fendler, J. H. *Chem. Eng. News* **1984**, *Jan. 2*, *62*, 25–38.

0002-7863/84/1506-8086$01.50/0